THE INFLUENCE OF SPECIMEN GEOMETRY ON STABLE CRACK GROWTH FOR A HIGH STRENGTH STEEL

H.-J. Kaiser and K. E. Hagedorn

Max-Planck-Institut für Eisenforschung, Max-Planck-Straße 1, 4000 Düsseldorf, W.-Germany

ABSTRACT

To investigate the influence of specimen geometry on the R-curve behaviour of a high strength steel 30CrNiMo8, fracture mechanics experiments were carried out on compact tension specimens with variable thickness, width and crack length. Different methods were applied to characterize the crack growth resistance for elastic-plastic material behaviour. It is described in terms of J-integral and effective K-values according to the ASTM recommendation E 561. The influence of specimen dimensions on the R-curve and the critical values of the elastic-plastic fracture mechanics parameters at the onset of crack growth and at maximum load is discussed. The R-curve using compliance-indicated effective crack growth was found to be independent of specimen width and crack length. Instability predictions for different geometries were made using this R-curve.

KEYWORDS

Fracture properties; stable crack growth; R-curves; elastic-plastic fracture mechanics; crack length measurement; instability.

INTRODUCTION

Stable crack growth is a phenomenon generally preceding the failure of structural materials in the upper transition-temperature range. To characterize material toughness from crack initiation up to specimen failure, the R-curve concept has been developed (Srawley and Brown, 1965). It describes the rise in crack growth resistance with increasing crack growth. Its technical use, i. e. the transfer of R-curves of small specimens to large specimens and structural components, is only possible if the influence of specimen geometry on stable crack growth is known. For linear-elastic material behaviour, the investigations of several authors (Krafft and co-workers, 1961; Schwalbe, 1977; Setz and Schwalbe, 1979) have found the R-curve to be independent of specimen dimensions except specimen thickness. However, steels are generally used at temperatures near the upper shelf transition-

temperature range where linear-elastic concepts are no longer applicable. Recently, attempts have been made to extend the R-curve concept to elastic-plastic material behaviour by using yielding fracture mechanics concepts. The purpose of this investigation was to derive R-curves in terms of different elastic-plastic fracture mechanics parameters and to study the influence of specimen geometry on the R-curve behaviour.

EXPERIMENTAL METHODS

Fracture mechanics experiments were carried out on an electro-slag-remelted high strength steel 30CrNiMo8 having a room temperature yield strength of 850 N/mm². The tests were conducted on compact tension (CT) specimens of various dimensions. The specimen thickness B ranged from 5 to 50 mm. At a constant thickness of 10 mm the specimen width W was varied between 25 and 100 mm and the ratio of crack length to specimen width a/W from 0.3 to 0.7. The experiments were carried out at 0°C where nearly all specimens displayed slow-stable crack growth up to and beyond the attainment of maximum load without any of the "pop-in" behaviour that occurred at lower temperatures.
To monitor the stable crack growth, DC potential drop equipment was used. The potential drop at the crack tip was measured and for temperature-compensation divided by a reference potential measured on the specimen surface beside the crack (Hagedorn and Rüdiger, 1977). The amplified, filtered and divided output signal of the potential drop device U_{out} was recorded together with the load line displacement (see Fig. 1). A distinct increase in the slope of the U_{out}-load line displacement curve was taken as the point for crack growth initiation. This point is indicated in Fig. 1 by an arrow.

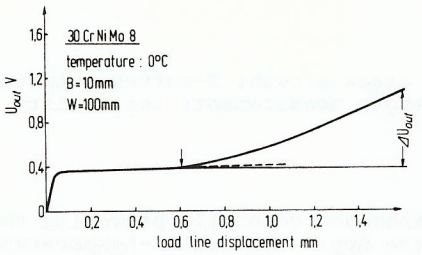

Fig. 1. Typical record of the potential drop device output signal U_{out} versus load line displacement.

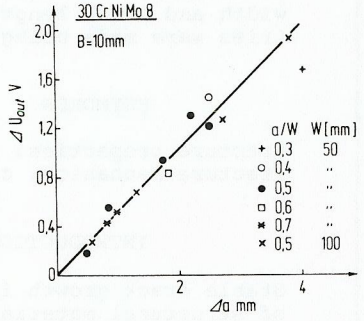

Fig. 2. Calibration curve of the potential drop device ΔU_{out} versus crack extension Δa for 10 mm thick CT-specimens.

Figure 2 shows a calibration curve of the potential drop device for specimens of different widths and a/W ratios. The curve was obtained by loading the specimens to maximum load or some lower displacement levels. After marking the fracture surfaces by a heat-tinting treatment the specimens were fractured in liquid nitrogen. ΔU_{out} represents the difference in the output signal from the initiation of stable crack growth to the end of loading. The crack growth Δa was evaluated by measuring the crack extension at nine points along the crack front and averaging to give mean values. A linear regression line can be drawn through the calibration points of the different sized specimens. For the specimen with a/W = 0.3 the reference potential amplification was changed and thus this point deviates from the regression line. Different slopes of the potential calibration curves were only obtained if the specimen thickness was varied (Kaiser and Hagedorn, 1980).

To characterize the crack growth resistance for elastic-plastic material behaviour, yielding fracture mechanics concepts were applied. J-integral values, respectively J resistance values J_R, were evaluated as proposed by Clarke and Landes (1979). For a/W ratios greater than 0.5 the expression

$$J = \frac{2A}{B(W-a)} \quad \frac{1+\alpha}{1+\alpha^2} \qquad (1)$$

was used, where A = area under the load-displacement curve and

$$\alpha = \sqrt{\left(\frac{2a_0}{W-a}\right)^2 + 2\left(\frac{2a_0}{W-a}\right) + 2} - \left(\frac{2a_0}{W-a} + 1\right)$$

(see Clarke and co-workers, 1978).

The analysis of Merkle and Corten (1974) that accounts for the tension component in the compact specimen was used to determine J for a/W ratios less than 0.5.

Values for the crack opening displacement δ were also calculated using the extrapolation technique according to the British standard BS-5762-1979.

Another way of obtaining an elastic-plastic R-curve is given in the ASTM recommendation E 561-76T. In accordance with this recommendation R-curves were plotted in terms of effective stress intensity factors K_R versus physical crack extension Δa_{phys} or effective crack extension Δa_{eff} where the effective crack length was determined from the load-displacement diagram and a calibration curve for the elastic specimen compliance.

RESULTS

The influence of thickness on the R-curves of 100 mm wide CT-specimens in terms of J_R and K_R versus Δa is shown in Figs. 3 and 4. R-curves in terms of δ-Δa are discussed elsewhere (Kaiser and Hagedorn, 1980) and not in this paper because they yield a very similar picture as the J_R-Δa curves. Δa is the average physical crack growth calculated from the potential drop measurement.
The different elastic-plastic methods produce a similar picture of the rise in crack growth resistance with stable crack extension. It was found that for specimens with a/W = 0.5, R-curves in terms of the effective stress intensity factor K_R versus crack growth Δa are equivalent to J-integral based R-curves up to the attainment of maximum load (Kaiser and Hagedorn, 1980), as reported by McCabe and Landes (1978). The stable crack growth begins well before maximum load at about the same J_i-values for the different thicknesses except for the 5 mm thick

specimen where it seems to begin at lower values. The rise in crack growth resistance with crack extension is larger for thinner specimens exhibiting more extensive plastic deformations. The J-integral and K_R-values at maximum load increase with decreasing specimen thickness. The slight decrease for the 5 mm thick specimen is probably due to experimental scatter, since a larger maximum load value was observed for another specimen of the same size.

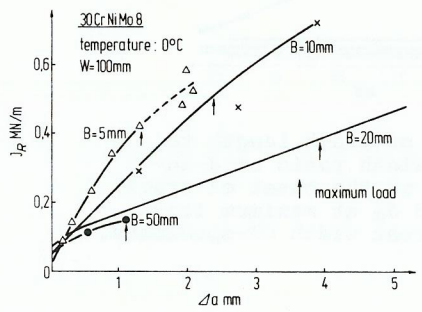

Fig. 3. Effect of specimen thickness on R-curve behaviour J_R-Δa for 100 mm wide CT-specimens.

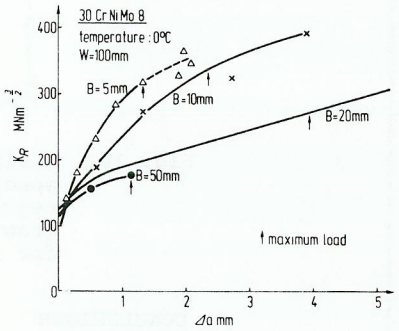

Fig. 4. Effect of specimen thickness on R-curve behaviour K_R-Δa for 100 mm wide CT-specimens.

To check the crack length calculation obtained by the potential drop measurement, several specimens of various thicknesses and widths were loaded up to different displacement values and then unloaded to mark the crack growth by a heat-tinting treatment. The points of the R-curves received by this multiple specimen technique are marked in Figs. 3 to 5. The points are well matched to the R-curves based on the crack extension measurement with the potential drop device.

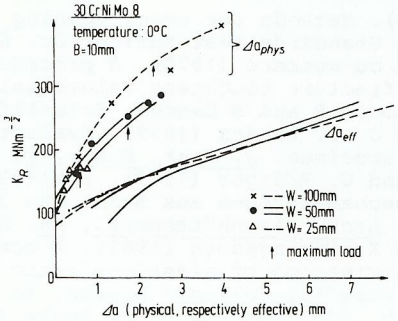

Fig. 5. Effect of specimen width on R-curve behaviour K_R-Δa_{phys} and K_R-Δa_{eff} for 10 mm thick CT-specimens.

The influence of specimen width on the R-curves determined according to the ASTM recommendation E 561 is shown in Fig. 5. The crack growth resistance K_R is plotted against the physical crack growth determined by the potential drop technique and also against the effective crack growth calculated from the load-displacement record and a calibration curve for the elastic specimen compliance. A scatterband of five experiments is drawn for the 50 mm wide specimens. A potential drop measurement was not conducted for the 25 mm wide specimens. The R-curves in terms of K_R versus Δa_{phys} are within one scatterband for all specimen widths in the initial, steeply-rising part. But after some amount of crack extension, probably when a certain upper limit of the degree of plasticity is exceeded, the R-curves are no longer independent of specimen width and an increasing specimen width results in a steeper slope in the R-curves. However, the R-curves do coincide for the three specimen widths if plotted in terms of K_R versus effective crack growth. For small Δa_{eff}-values the scatterband of the K_R-Δa_{eff} curves is very wide because small variations in the establishment of the linear initial part of the load-displacement diagram yield large errors in Δa_{eff}. But a very good coincidence of the R-curves of the specimens of different width exists for higher Δa_{eff}-values.

Furthermore the influence of specimen width on the values of the elastic-plastic fracture mechanics parameters at maximum load can be seen from Fig. 5. The K_R-values and also the δ- and J-integral values at maximum load, not shown in this figure, clearly increase with specimen width.

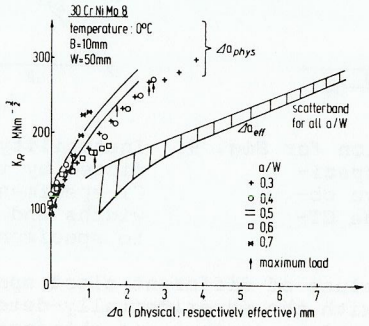

Fig. 6. Effect of crack length to specimen width ratio on R-curve behaviour K_R-Δa_{phys} and K_R-Δa_{eff} for 10 mm thick CT-specimens.

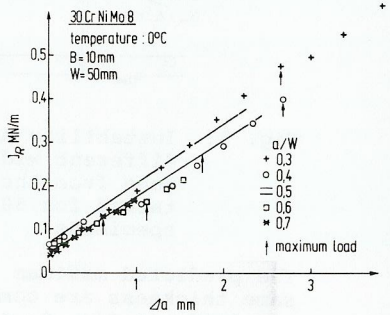

Fig. 7. Effect of crack length to specimen width ratio on R-curve behaviour J_R-Δa for 10 mm thick CT-specimens.

Figure 6 shows R-curves according to the ASTM-recommendation E 561 for 50 mm wide specimens with different a/W ratios. The R-curves in terms of K_R versus Δa_{phys} are within one small scatterband in the initial part irrespective of the various a/W ratios. Though there are slight differences between the R-curves of the different sized specimens, the scatterband is not very large up to the attainment of maximum load and a systematic influence of the a/W ratio on the course of the R-curve was not observed.

A very good coincidence of the R-curves for different a/W ratios is again established when plotted in terms of K_R versus effective crack growth. After an initially wide spread, all R-curves are within one shaded scatterband for higher Δa_{eff}-values. A small scatterband of the R-curves for the different a/W ratios can also be obtained when the curves are plotted in terms of J_R versus physical crack growth Δa (Fig. 7). They coincide very well up to and beyond the attainment of maximum load.

A critical test of R-curve results is to predict instability (maximum) loads and to compare them with the experimentally-determined values. In Figure 8 an average R-curve, derived from five experiments with 10 mm thick and 50 mm wide specimens by fitting with a second order polynomial, is shown in terms of K_R versus Δa_{eff} together with crack driving curves for specimens of different width fulfilling the tangency condition for instability. All plasticity effects are contained within the R-curve in the use of a_{eff} to calculate K_R and in the use of Δa_{eff} on the abscissa. The crack extension drive is totally elastic.

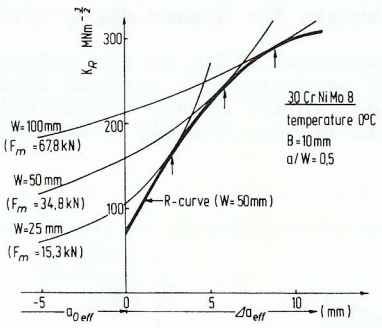

Fig. 8. Instability prediction for different width CT-specimens from the R-curve obtained for 50 mm wide CT-specimens.

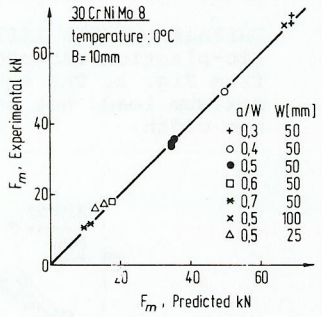

Fig. 9. Instability loads F_m predicted by the R-curve for CT-specimens of different widths and crack length to specimen width ratios.

The predicted maximum load values of different sized specimens of the same thickness are compared with the experimentally-determined maximum loads in Fig. 9. A remarkable agreement was obtained for all specimen widths and a/W ratios indicating that the R-curve concept is also applicable for elastic-plastic material behaviour. But to prove its general applicability in the elastic-plastic regime, further experiments have to be carried out on steels of different strength.

Finally, the influence of crack length to specimen width ratio a/W on the critical J-integral values is shown in Fig. 10. A systematic influence of the a/W ratio on the J_i-values at crack growth initiation was not observed for both specimen widths. The narrowly spread J_i-values for the 50 mm wide specimens fall into the scatterband for the 100 mm wide specimens. A distinct increase of the J_m-values at maximum load with decreasing a/W ratio can be seen. As mentioned above, the specimen width also has a striking influence on the J-integral values at maximum load.

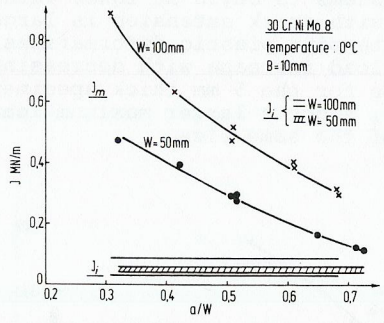

Fig. 10. Influence of crack length to specimen width ratio on J-integral J_i at the onset of crack growth and J_m at maximum load for different width CT-specimens.

CONCLUSIONS

Different elastic-plastic methods were used to derive elastic-plastic R-curves for different sized specimens of the high strength steel 30CrNiMo8. A remarkable influence of specimen thickness on R-curve behaviour was observed. An influence of specimen width on the R-curve plotted in terms of the effective stress intensity factor K_R versus physical crack growth was also found after a certain rise in crack growth resistance. However, R-curves in terms of K_R versus effective crack growth were found to be independent of specimen width and a/W ratio enabling a precise prediction of instability loads for different specimen geometries, indicating the applicability of R-curve methods also in the elastic-plastic regime.

REFERENCES

BS 5762:1979 (1979). Methods for crack opening displacement (COD) testing. British Standards Institution, Gr. 6.

Clarke, G. A., and co-workers (1978). A procedure for the determination of ductile fracture toughness values using J integral techniques. Westinghouse R and D Center, Scientific Paper 78-1D3-JINTF-P2.

Clarke, G. A., and J. D. Landes (1979). Evaluation of the J integral for the compact specimen. J. Test. Eval., 7, No. 5, 264-269.

Hagedorn, K. E., and U. Rüdiger (1977). Ermittlung von Ermüdungsrißlängen in Bruchmechanikproben aus Stahl RSt 37-2 mit dem Potentialsondenverfahren. Arch. Eisenhüttenwes., 48, No. 9.

Kaiser, H.-J., and K. E. Hagedorn (1980). A comparison of different methods for determination of elastic-plastic R-curves. Proc. 3rd Eur. Coll. Fracture, Imperial College, London, to be published.

Krafft, J. M., A. M. Sullivan and R. W. Boyle (1961). Effect of dimensions on fast fracture instability of notched sheets. Proc. Crack Propagation Symp., College of Aeronautics, Cranfield, U. K..

McCabe, D. E., and J. D. Landes (1978). Elastic-plastic R-curves. Trans. ASME, J. Engng. Mat. Tech., 100, 258-266.

Merkle, J. G., and H. T. Corten (1974). A J-integral analysis for the compact specimen, considering axial force as well as bending effects. ASME, Paper No. 74-PVP-33.

Schwalbe, K. H. (1977). Influence of stress state on static crack growth in AlZnMgCu0.5. Engng. Fracture Mech., 9, 557-583.

Setz, W., and K. H. Schwalbe (1979). R-Kurve und Restfestigkeit bei dünnen Querschnitten. Ber. 11. Sitzung A. K. Bruchvorgänge, Stuttgart, DVM.

Srawley, J. E., and W. F. Brown Jr. (1965). Fracture toughness testing methods. In ASTM STP 381, Am. Soc. Test. Mats., pp. 133-198.